11-1-2012

On Pi-Stacking, CH/Pi, and Halogen Bonding in Halobenzene Clusters: Resonant 2-Photon Ionization Studies of Chlorobenzene

Lloyd Muzangwa
Marquette University

Silver Nyambo
Marquette University

Brandon Uhler
Marquette University

Scott Reid
Marquette University, scott.reid@marquette.edu

Published version. *The Journal of Chemical Physics*, Vol. 137, No. 184307 (November 2012): 1-9.DOI.

On π-stacking, C-H/π, and halogen bonding interactions in halobenzene clusters: Resonant two-photon ionization studies of chlorobenzene

Lloyd Muzangwa, Silver Nyambo, Brandon Uhler, and Scott A. Reid
Department of Chemistry, Marquette University, P.O. Box 1881, Milwaukee, Wisconsin 53201-1881, USA

(Received 30 August 2012; accepted 12 October 2012; published online 12 November 2012)

Noncovalent interactions such as hydrogen bonding, π-π stacking, CH/π interactions, and halogen bonding play crucial roles in a broad spectrum of chemical and biochemical processes, and can exist in cooperation or competition. Here we report studies of the homoclusters of chlorobenzene, a prototypical system where π-π stacking, CH/π interactions, and halogen bonding interactions may all be present. The electronic spectra of chlorobenzene monomer and clusters $(Clbz)_n$ with $n = 1$-4 were obtained using resonant 2-photon ionization in the origin region of the S_0–S_1 ($\pi\pi^*$) state of the monomer. The cluster spectra show in all cases a broad spectrum whose center is redshifted from the monomer absorption. Electronic structure calculations aid in showing that the spectral broadening arises in large part from inhomogeneous sources, including the presence of multiple isomers and Franck-Condon (FC) activity associated with geometrical changes induced by electronic excitation. Calculations at the M06-2x/aug-cc-pVDZ level find in total five minimum energy structures for the dimer, four π-stacked structures, and one T-shaped, and six representative minimum energy structures were found for the trimer. The calculated time-dependent density functional theory spectra using range-separated and meta-GGA hybrid functionals show that these isomers absorb over a range that is roughly consistent with the breadth of the experimental spectra, and the calculated absorptions are redshifted with respect to the monomer transition, in agreement with experiment. Due to the significant geometry change in the electronic transition, where for the dimer a transition from a parallel displaced to sandwich structure occurs with a reduced separation of the two monomers, significant FC activity is predicted in low frequency intermolecular modes. © *2012 American Institute of Physics*. [http://dx.doi.org/10.1063/1.4765102]

I. INTRODUCTION

Noncovalent interactions of various types, such as hydrogen bonding, π-π stacking, CH/π interactions, and halogen bonding play a key role in influencing chemical reactivity and molecular structure,[1–10] in molecular recognition and binding,[11–16] and in the structure, stability, and dynamic properties of biomolecules.[17–22] Noncovalent forces are critical in determining the secondary, tertiary or quaternary structure of large molecules, and thus their macromolecular function.[19,20,22–25] Understanding the relative magnitude of these various types of interactions is important, particularly as they may exist in cooperation or competition,[23,26–29] and this has been the target of intense experimental and theoretical effort.[17,30–42] In this regard, mono-substituted halobenzene clusters are prototypical systems in which different noncovalent interactions may be operative, including π-π stacking,[32,40,41,43–50] CH/π,[18,40,51] and halogen bonding interactions, illustrated in Figure 1.[3,15,51–58]

Simple aromatic dimers involving benzene and toluene have long been proposed as model systems for understanding π-π stacking interactions in proteins,[24,59] and are also prototypes for exploring the relative importance of π-π stacking and CH/π interactions.[21] The story of the benzene dimer, in particular, is one of controversy and intense debate, with respect to the relative energies of parallel (π-stacked) and T-shaped (CH/π) structures.[43,44] State-of-the-art single reference [CCSD(T)/CBS] calculations by Sinnokrot and Sherrill show that parallel displaced and T-shaped structures are nearly isoenergetic, with the symmetric D_{6h} sandwich structure lying 1 kcal/mol higher in energy.[39] Experimental studies of aromatic homo- and heteroclusters have exploited a range of techniques, with mass-selected resonance ionization methods at the forefront. Thus, Bernstein and co-workers reported the first resonant 2-photon ionization (R2PI) spectra for toluene dimer through the S_1 state, which showed two features that were significantly broadened with respect to the monomer absorption.[30,31,60] These two features were attributed to different isomers, and the presence of at least two different isomers was confirmed in subsequent two-color hole-burning spectra.[61] Similar studies using R2PI and zero-kinetic energy (ZEKE) spectroscopy have been reported on substituted benzene dimers, including dimers of fluorobenzene,[62–69] chlorobenzene,[58,70] phenol, aniline,[71–74] and others.[39,75]

Building upon the seminal studies of Bernstein and others, Musgrave and Wright recently reported R2PI spectra of mass-selected toluene homoclusters $(Tol)_n$ up to $n = 8$,[60] and parafluorotoluene clusters $(pfTol)_n$ up to $n = 11$.[76] The striking result of this work was that the spectra of the higher order clusters were very similar to that of the dimer. The authors proposed a model by which the favored (π-stacked) binding motif of the dimer formed the core of higher order clusters, leading to a "dimer chromophore" that was responsible for

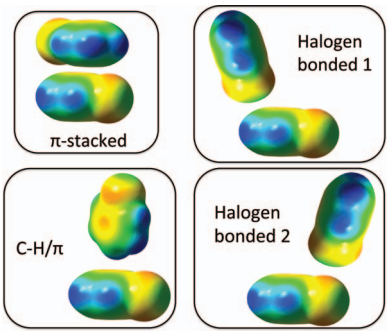

FIG. 1. Schematic of possible non-covalent interactions in halobenzene dimers. The electrostatic potential surface of chlorobenzene calculated at the M06-2x/aug-cc-pVDZ level is shown.

the electronic spectrum of higher order clusters. This explanation was supported by subsequent measurements of the ionization potential of mass-selected toluene clusters in a molecular beam.[59] Here a reduction in the ionization potential of the dimer relative to the monomer was found, consistent with the participation of a π-stacked dimer where the cationic charge could be delocalized over both rings. Relative to the dimer, the ionization potential of the trimer and tetramer was unchanged, which was taken as evidence against the existence of fully π-stacked clusters in the beam.

The S_0–S_1 spectroscopy and dissociation of halobenzenes have been extensively studied by R2PI and related methods;[77–82] however, relatively few R2PI spectroscopic studies of clusters of mono-substituted benzenes have been reported.[62–70] Chlorinated aromatic compounds are important pollutants,[83] however, the nature of intermolecular interactions in chlorobenzene clusters are still unclear and relatively few studies have been reported.[58] Lu *et al.*, conducted a study of chlorobenzene and chlorobenzene-benzene complexes by R2PI in a reflectron time-of-flight (TOF) mass spectrometer (MS).[70] For the chlorobenzene dimer, in the region of the S_0–S_1 ($\pi\pi^*$) origin two distinct and, in comparison to the monomer absorption, very broad features were observed; one blueshifted relative to the monomer absorption and the other redshifted. The redshifted absorption was assigned to a T-shaped dimer, and the blueshifted absorption to a parallel-displaced (π-stacked) dimer. Support for the assignment of these absorptions to distinct species was provided in the carrier gas and backing pressure dependence of the relative intensities. In particular, it was found that the blueshifted absorption increased in intensity when using Ar rather than He as the carrier gas, and at higher backing pressures. The binding energy of the chlorobenzene dimer, determined using the breakdown method, was determined to be 14.5 ± 1.0 kJ/mol.[70]

The chlorobenzene clusters $(Clbz)_n$ with n = 2-4 have recently been studied using ultrafast spectroscopy in a supersonic beam.[58] Following excitation of the $S_1(\pi$-$\pi^*)$ states at 267 nm, the decay dynamics of the clusters was found to exhibit multiple time scales, reflecting in part cracking of higher order clusters into the measured channel. However, an intrinsic biexponential decay was found for all clusters. The fast (~170 fs) component was found to decrease with cluster size, and was attributed to internal conversion to the S_0 state. In contrast, the slow component (~1 ns), which was attributed to subsequent dissociation of the hot S_0 molecules, *increased* with cluster size. This was explained from the viewpoint of a statistical process, where the timescale for reaction correlates with the available phase space in the reacting molecule.

The present work highlights the study of competitive non-covalent forces in chlorobenzene clusters, using R2PI spectroscopy in concert with electronic structure calculations using density functional theory (DFT) and post-Hartree–Fock (MP2) methods and correlation consistent basis sets. Motivating this work is the desire to understand the nature of the competitive non-covalent interactions in the monohalobenzenes, which in comparison to benzene or toluene includes also the potential for halogen bonding interactions between the σ-hole of a halogen on one fragment and the halogen or π-system on the other (Figure 1).

II. EXPERIMENTAL AND COMPUTATIONAL METHODS

Our experiments utilized a linear TOFMS coupled with a supersonic molecular beam source based upon a General Valve pulsed nozzle. A schematic of the experimental apparatus is shown in Figure S1 in the supplementary material.[84] A 1% mixture of the chlorobenzene precursor in He, generated by passing the high purity gas over a sample of chlorobenzene held in a temperature controlled bath, at a total pressure of typically ~1-2 bar was expanded from the 1.0 mm diameter nozzle of the pulsed valve, and passed through a 1.0 mm diameter skimmer into the differentially pumped flight tube of a 1-m linear TOFMS, described in some detail in our previous work.[85–87] The flight tube was evacuated by a 250 L/s turbomolecular pump, with a gate valve used to isolate the detector, which was kept under vacuum at all times. The main chamber was evacuated with a water-baffled diffusion pump (Varian VHS-4). With the nozzle on, typical pressures were ~5 × 10^{-5} mbar (main chamber) and ~1 × 10^{-6} mbar (flight tube). The background pressure in the flight tube could be lowered further by liquid nitrogen cooling of the vacuum shroud; however, this was not required in the present experiments.

Ionization was initiated by a 1+1 R2PI scheme, with laser light near 267 nm generated from frequency doubling in a BBO crystal the output of a dye laser (Lambda-Physik, Scanmate 2E), pumped by the third harmonic of an Nd:YAG laser (Continuum NY-61). The laser was operated on a C540A dye, giving typical output pulse energies of ~0.5 mJ in the doubled beam, which was loosely focused with a 1.0 m focal length plano-convex lens into the chamber. In some experiments, 1+1′ resonant 2-color 2-photon ionization (R2C2PI) was employed, with the 266 nm output of a second Nd:YAG system (Continuum Minilite II) introduced as the ionization laser. In these experiments, the focusing lens in the doubled dye beam path was removed to reduce the contribution from 1+1 signal, and the ionization laser was loosely focused with a 0.5 m focal length lens. The delay between the lasers and molecular beam was controlled by an eight-channel digital delay generator (BNC 565).

Ions were extracted and accelerated using a conventional three-plate stack, with the repeller plate typically held at 2100 V, the extractor plate at 1950 V, and the third plate at

ground potential (Figure S1 of the supplementary material).[84] The ions traversed a path of 1 m prior to striking a dual chevron microchannel plate detector. The detector signal was amplified (×25) using a fast preamplifier (Stanford Research SRS445A), and integrated using a boxcar system (Stanford Research SRS250) interfaced to a personal computer. An in-house LabVIEW program controlled data acquisition and stepped the laser wavelength; typically, the signal from twenty laser shots was averaged at each step in wavelength.

To support our experimental findings, electronic structure calculations were performed using the GAUSSIAN 09 software package on the MU Pere cluster.[88] Full geometry optimizations were carried out using DFT (M06-2x) and post-Hartree–Fock (MP2) methods using an aug-cc-pVDZ basis set. Our choice of method was dictated in part by the extensive computational studies, notably those of Sherrill and co-workers, on related systems,[17,34,39] where the performance of DFT methods in combination with various correlation consistent basis sets has been extensively benchmarked against high level post-Hartree–Fock *ab initio* single reference methods. It was shown that the Minnesota meta-GGA (generalized gradient approximation) hybrid functional M06-2x, among other methods, provides a good cost to performance ratio,[34] and the aug-cc-pVDZ basis set performs well in calculating the counterpoise correction.[34] Zhao and Truhlar have shown that M06-2x performs well in describing the energies of π-stacking interactions.[89] In this work, our calculated binding energies were corrected for zero point energy (ZPE), and the counterpoise method was employed to correct for basis set superposition error.

Time-dependent DFT (TDDFT) methods are quite popular for modeling electronically excited states, and it is well appreciated that local exchange functionals perform poorly for states involving significant charge transfer.[90] Thus, in this work we employed TDDFT methods using range-separated hybrid and meta-GGA hybrid functionals to calculate the electronic spectra of the clusters and the optimized geometry of the S_1 states. Methods employed included the range-separated hybrid functional ωB97X-D,[91] the meta-GGA hybrid functionals M06 and M06-2x,[89] and CAM-B3LYP,[92,93] all with an aug-cc-pVDZ basis set. The performance of the ωB97X-D and M06-2x methods for electronic excitations, including Rydberg and charge transfer excitations, have recently been benchmarked by Head-Gordon and co-workers.[94]

III. RESULTS AND DISCUSSION

Representative R2PI spectra of the chlorobenzene monomer and chlorobenzene clusters $(Clbz)_n$ with n = 2-4 in the region of the origin band of the monomer S_0–S_1 ($\pi\pi^*$) transition are displayed in Figure 2. The electronic spectroscopy of the chlorobenzene monomer is well known and has been extensively studied previously by other groups using both R2PI and laser induced fluorescence spectroscopy.[70,95–98] Note also that the size range of clusters that we observe is similar to that found in the prior ultrafast experiments, where a similar source was used.[58] From Figure 2, it is apparent that the clusters uniformly exhibit much broader absorption features than the monomer, yet the

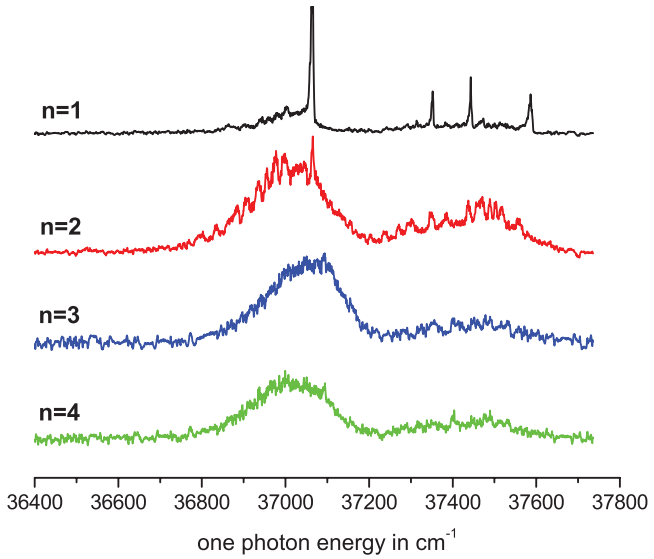

FIG. 2. Resonant two-photon ionization (R2PI) spectra of mass-selected chlorobenzene monomer and clusters $(Clbz)_n$ with n = 2-4.

spectra of different clusters in the range n = 2-4 are similar. The spectra for the clusters show a maximum absorption at lower energy (i.e., are redshifted) with respect to the monomer peak. As noted in the introduction, the broad absorption features that we observe here for the clusters of chlorobenzene have previously been observed for related systems, including toluene dimer, fluorobenzene dimer, and mixed halobenzene-benzene dimers.[30,31,70,75] We consider several explanations for the source of this broadening.

An obvious explanation for the similarity of the cluster spectra is cracking of larger clusters, giving rise to signals in the mass channels of smaller clusters. Indeed, some cracking is clearly apparent in the monomer spectrum shown in Figure 2, as a weak broad background underlying the strong sharp features of the monomer. Expanding this spectrum and overlaying with the dimer spectrum shows strong similarities (Figure S2), indicating that some of the monomer signal arises from cracking of the dimer into the monomer mass channel. In order to test for the contribution of cracking to the observed dimer spectrum, we lowered the concentration of chlorobenzene in mixture below 1% by cooling the sample bath, which effectively reduced the concentration of higher order clusters. At a point at which the trimer signal can barely be observed, the dimer spectrum is unchanged, retaining its very broad appearance (Figure S3).

A second explanation for the broadness in the cluster spectra is the presence of different isomers, which might absorb at different wavelengths. Indeed, a motivating aspect of this study was the exploration of the relative importance of different non-covalent interactions in these clusters. This was examined using calculations at the M062x and MP2 levels with an aug-cc-pVDZ basis set, with geometry optimizations initiated from a variety of starting geometries that loosely corresponded to π-stacked, C-H/π, and halogen-bonded structures (Figure 1). In all, five minimum energy structures (D1-D5) were found for the chlorobenzene dimer, and the optimized (M06-2x/aug-cc-pVDZ) structures are shown in

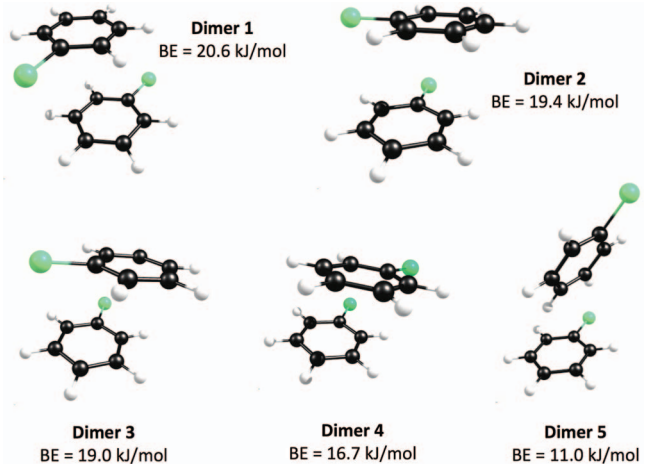

FIG. 3. Optimized structures (D1-D5) for the chlorobenzene dimer, calculated at the M06-2x/aug-cc-pVDZ level of theory. Binding energies are counterpoise and ZPE corrected.

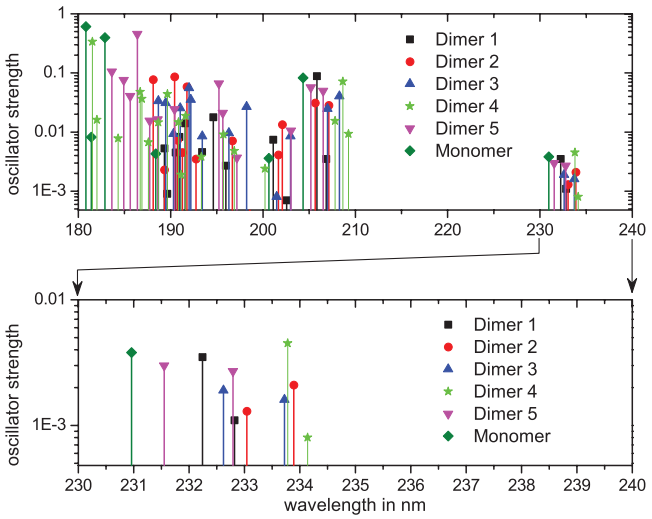

FIG. 4. Calculated TDDFT (TDM06-2x/aug-cc-pVDZ) spectra of the chlorobenzene dimers shown in Figure 3. The lower panel shows an expanded view of the lowest energy transitions.

Figure 3, together with the calculated binding energies, which were counterpoise and ZPE corrected. Dimers D1-D4 are π-stacked with a parallel-displaced structure, consistent with previous findings for related systems.[17,34,41,42] In these structures the planes of the two monomers are separated by ~3.3 Å, so that the two Cl atoms are not in close van der Waals contact. This gives rise to four different π-stacked isomers, differing in the relative orientation of the Cl atoms (Figure 3) with calculated binding energies between ~17 and ~20 kJ/mol. In addition to the π-stacked isomers, a T-shaped isomer (D5) was also found (Figure 3), with a calculated binding energy roughly one-half that of the π-stacked isomers. No local minima corresponding to halogen-bonded structures were found.

Comparing the M06-2x/aug-cc-pVDZ results with other calculations, we find that the calculated MP2/aug-cc-pVDZ binding energy of dimer 1 (D1) is ~27 kJ/mol. This difference is not surprising, as it is well known that the MP2 method tends to over-estimate the strength of non-covalent interactions, particularly in cases dominated by dispersion.[99,100] In comparison, a counterpoise corrected CCSD(T)//M06-2x/aug-cc-pVDZ calculation using ZPE corrections at the M06-2x/aug-cc-pVDZ level yields a binding energy of 13.8 kJ/mol, which suggests that the M06-2x results are also overestimates. The coupled cluster prediction is in excellent agreement with the experimentally determined binding energy of the dimer (14.5 ± 1.0 kJ/mol).[70]

The trends in the calculated binding energies give some insight into the importance of dipole-dipole coupling in this system. For example, the π-stacked structure (D1) with the dipoles opposed is the global minimum according to our calculations, as expected, with a binding energy ~25% larger than the structure (D4) where the dipoles are nearly aligned. The importance of the dipole-dipole interaction is also shown in the larger (×2) calculated binding energy of the π-stacked vs. T-shaped (CH/π) structure (Figure 4); as noted above, for the benzene dimer the calculated binding energies are similar. It is also instructive to compare experimental binding energies, determined using the breakdown method, for the chlorobenzene homodimer (14.5 ± 1.0 kJ/mol) and chlorobenzene-benzene heterodimer (13.5 ± 1.0 kJ/mol), relative to the benzene homodimer (6.8 ± 1.0 kJ/mol).[70] The binding energies for the former are nearly twice that of the latter, indicating that dipole-dipole and dipole-induced dipole interactions contribute significantly to the overall binding in these complexes.

The calculated TDDFT (TDM06-2x/aug-cc-pVDZ) spectra of the chlorobenzene dimers D1-D5 and monomer are shown in Figure 4, referenced to the numbering scheme given in Figure 3 and plotted as stick spectra. Quantitatively, the TDDFT calculations overestimate the position of the S_1 state of the monomer; however, we expect that trends in these calculations should be valid, and this is addressed further below. The calculated spectra of the dimers show two absorptions split by the exciton coupling. In the exciton picture, the excited state wavefunction of the dimer is written as a superposition of localized excitations on each monomer, and the coupling between the two chromophores leads to a splitting of the monomer absorptions. Such coupling will typically involve both dipole-dipole and exchange interactions, and is dependent upon the relative orientation of the transition dipoles. Indeed, the splitting of dimer D4 is the smallest among the π-stacked systems, consistent with this notion.

Beyond the exciton splittings, in all the dimers the calculated electron transitions are predicted to lie to lower energy (i.e., are redshifted) compared to the monomer absorption, and the absorption lying closest to the monomer transition is that for the "free" chlorobenzene in the T-shaped dimer. The calculated spectra of the various isomers occur over a range that, when scaled to reflect the overestimation of the transition energy, is of an order roughly similar to that observed experimentally. In order to assess the dependence of these results on the method used, we carried out additional calculations on the chlorobenzene monomer and dimer D1, used as a representative example. These employed a wider range of functionals, including ωB97X-D,[91] M06,[89] and CAM-B3LYP,[92,93] and the results are shown in Figure S4. The trends observed in these

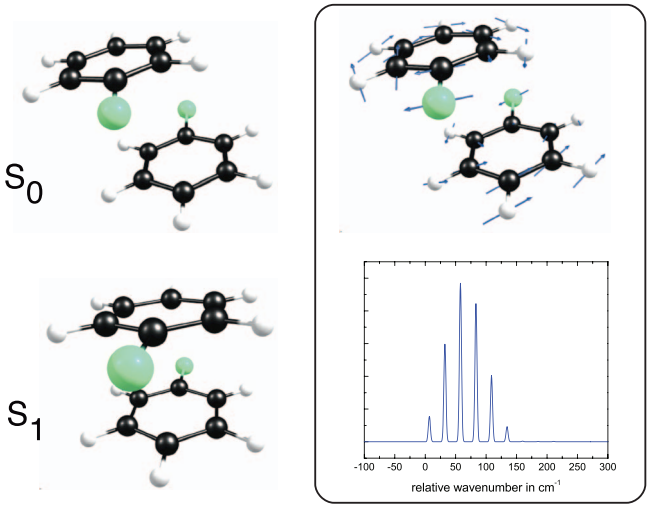

FIG. 5. (Left) Optimized structures of the ground and lowest energy excited electronic state of chlorobenzene dimer 1. (Right) Ground state displacements for the lowest energy torsional mode, and simulated spectrum showing the FC activity in this mode in the S_0–S_1 transition of the dimer, as described in the text.

calculations are consistent, with the transitions of the dimer lying to the red (lower energy) of the monomer transition. There is some variation in the exciton splitting and in the magnitude of the calculated redshift, with the ωB97X-D and CAM-B3LYP results displaying smaller shifts as compared with M06 and M06-2x.

In addition to inhomogeneous broadening arising from the different isomers in the beam, additional features are expected for each isomer arising from vibrational structure based upon the Franck-Condon (FC) activity in the electronic transition. To model this, we optimized the structure of the lowest lying excited electronic state of dimer 1 (Figure 3) at the TDM06-2x/aug-cc-pVDZ level. The optimized structures of the ground and excited states of this dimer are shown in Figure 5; interestingly, the calculations predict a transition from a parallel-displaced structure in the ground state to a sandwich structure in the excited state, with the distance between the monomers decreasing from ~3.3 to ~3.0 Å. A sandwich structure was predicted for the equilibrium geometry of the lowest excited valence state of the benzene dimer.[101,102] As a result of this geometry change, significant FC activity is expected in low frequency torsional modes that involve displacement of the two monomer subunits; the vibrational displacements associated with the lowest frequency such mode ($\omega \sim 26$ cm^{-1}) in the ground state are shown in Figure 5. To simulate the vibronic spectrum, we incorporated the calculated vibrational frequency and mass-weighted cartesian displacements (i.e., *l*-matrices) of this mode in the ground and excited electronic states into a FC simulation that accounted for the effects of Duschinsky mixing. These calculations were performed using a routine in the PGOPHER program suite.[103] The calculated spectrum, Figure 5, shows significant FC activity in this mode. While this simulation is illustrative, in the sense that it is not meant to completely capture the vibrational structure in the spectrum and is based on a harmonic approximation which may be a poor description of these low frequency intermolecular modes,[66,67] it does suggest that additional features will arise from FC activity in the spectrum, which will further contribute to the observed broadening. Indeed, the vestiges of this structure appear in the measured dimer spectrum (Figure 2), which we did not attempt to model quantitatively due to the presence of multiple isomers. Given the low frequency of this and other intermolecular modes, hot-band structure may also be present.

Thus far we have neglected contributions from homogeneous broadening. In a related study of the complexes of 2-pyridone with substituted fluorobenzenes, Leutwyler and co-workers found that the complexes of partially fluorinated benzenes exhibited sharp spectra indicative of a hydrogen-bonded complex.[66,67] In contrast, the π-stacked complex with hexafluorobenzene exhibited a number of very broad features, which were explained in terms of vibronic structure in the low frequency intermolecular modes. Hole-burning experiments revealed the presence of two isomers, and indicated that the primary broadening mechanism in the spectra was homogeneous broadening. Indeed, the previous ultrafast experiments on chlorobenzene clusters reveal a bi-exponential decay with a short lifetime component on the order of ~200 fs.[58] Thus, while our analysis of the chlorobenzene dimer spectrum shows that the general features can be adequately explained by the presence of multiple isomers and vibrational activity in low frequency intermolecular motions, homogeneous broadening must also be a contributing factor. Hole-burning experiments will be needed to assess the relative contributions of homogeneous and inhomogeneous broadening to the spectrum.

Moving to the higher clusters, an important question is: *Why is the spectrum of the trimer and tetramer so similar to that of the dimer?* To answer this question, we calculated representative structures of the trimer at the M06-2x/aug-cc-pVTZ level. A total of six minimum energy trimer structures were found, (T1-T6), shown in Figure 6, which exhibit the same noncovalent interactions (π-π stacking, CH/π) found to be important in the dimer. The binding energies of these trimers, counterpoise and ZPE corrected, are referenced to

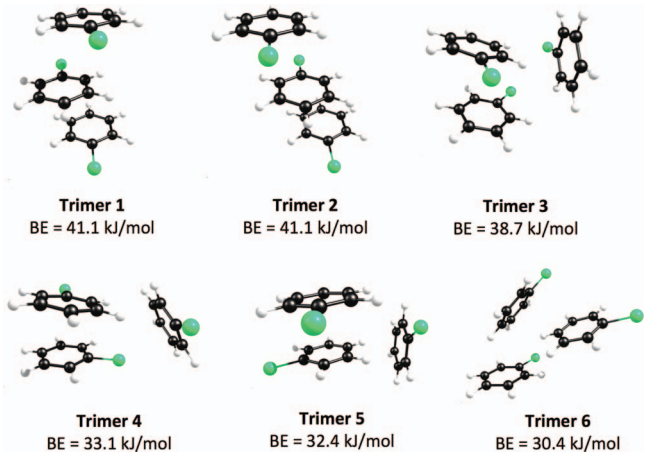

FIG. 6. Optimized structures (T1-T6) for the chlorobenzene trimer, calculated at the M06-2x/aug-cc-pVDZ level of theory. Binding energies are counterpoise and ZPE corrected, and are referenced to the energy of three separated monomers.

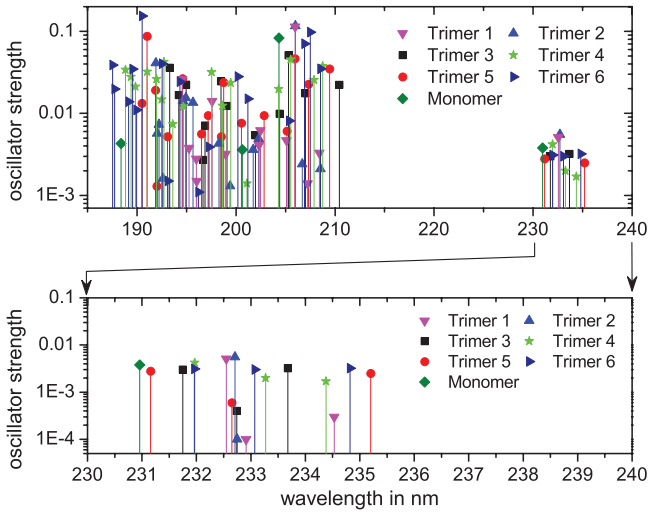

FIG. 7. Calculated TDDFT (TDM06-2x/aug-cc-pVDZ) spectra of the chlorobenzene trimers shown in Figure 5. The lower panel shows an expanded view of the lowest energy transitions.

the energy of three monomers. As Tauer and Sherrill have previously shown,[104] aromatic clusters do not exhibit significant nonadditive effects in their binding, and thus the binding energies (~40 kJ/mol) of the fully π-stacked trimers (T1 and T2) are roughly twice the energy of the π-stacked dimer. The remaining trimer configurations (T3 – T6) typically have a stacked dimer core, with the third monomer interacting with this core through CH/π interactions. These display BEs of 30-39 kJ/mol. It is important to note that many additional minimum energy structures for the trimer can be envisaged; however, the calculated structures shown in Figure 6 are considered to be representative. It is reasonable to expect that all of these isomers are present, to a varying degree, in our beam.

Figure 7 displays the calculated (TDM06-2x/aug-cc-pVDZ) spectra of trimers T1-T6. These spectra show three split transitions per trimer. As found for the dimers, the calculated transitions are all redshifted with respect to the monomer absorption. Importantly, the range over which these absorptions occur is very similar to that observed for the dimers (Figure 4), which suggest that the coupling between the chromophores is similar. Thus, the similarity of the dimer and trimer spectra is in part explained by the presence of multiple isomers, whose electronic spectra span a similar range.

As discussed in the Introduction, in order to explain the similarity of R2PI spectra for toluene and para-fluorotoluene clusters of different size, Wright and co-workers proposed that the favored (π-stacked) binding motif of the dimer formed the core of higher order clusters, leading to a dimer-based "chromophore."[76] Our results are not inconsistent with this picture, in that it is certainly true that a π-stacked dimer, being the most favorable binding motif, is found in the majority of optimized trimer structures (Figure 7). However, another way to view this is that the noncovalent interactions and interchromophore couplings in the dimer and trimer are similar, leading to shifts in the electronic absorptions that occur over a similar range (Figures 4 and 7), which gives rise to the similarity of the spectra. This, of course, could hold for larger clusters as well.

A dimer-based model of stacking in toluene clusters has also been invoked to explain the dependence of ionization potential on cluster size.[59] As noted above, a reduction in the ionization potential of the toluene dimer relative to the monomer was found, consistent with the participation of a π-stacked dimer where the charge is delocalized over both rings.[59] This suggests the importance of π-stacking in the dimer, and is consistent with our finding that 80% of optimized (calculated) chlorobenzene dimer structures contain this motif. In contrast, the ionization potential of the trimer and tetramer of toluene was found to be similar to the dimer, which was taken as evidence against the existence of the (lower energy) fully π-stacked clusters in the beam, and it was argued that the lack of relaxation in the beam favored formation of higher energy structures. Given the range of possible isomers, each present to an unknown degree and displaying an ionization potential dependent upon the degree of π-stacking, it is clear that the interpretation of ionization potential measurements made from single photon VUV excitation should be made with care.

Moving to the chlorobenzene tetramer ($n = 4$), we obtained a R2PI spectrum (Figure 2), which again was broad and redshifted compared to the monomer absorption, and similar to the spectrum of the dimer and trimer. Due to the computational resources required in characterizing even a representative set of the large number of potential isomeric structures, we made no effort to run electronic structure calculations for the tetramer. However, one can reasonably predict that the interactions observed in the dimer and trimer will also be important in the tetramer, and it is also reasonable to assume, based upon the analysis presented here, that the similarity of the tetramer spectrum to that of the dimer and trimer can be explained in part by the presence of multiple isomers.

Comparing our results with previous R2PI studies of the chlorobenzene dimer by Lu *et al.*,[70] we note that a feature observed to higher energy of the monomer origin was assigned in that work to the π-stacked dimer. We observe a shoulder on the dimer spectrum (Figure 2) at this position; however, our calculations predict that the highest energy dimer absorption is that for the T-shaped (not parallel displaced) isomer, and thus the blueshifted feature most probably reflects vibrational structure associated with the absorption of this isomer. Lu *et al.* found that the intensity of the blueshifted feature greatly increased when using Ar (rather than He) as backing gas, and further increased with an increase in backing pressure. It is possible that the different expansion conditions may favor formation of the higher energy T-shaped isomer, through an unknown mechanism. In this work we did not carry out experiments with Ar backing gas, to avoid contributions from van der Waals complexes of Ar and chlorobenzene. For their binding energy measurements, Lu *et al.* used He backing gas at a relatively low backing pressure, which would favor the redshifted (π-stacked) component. This is consistent with the very good agreement between the experimentally measured binding energy (14.5 ± 1.0 kJ/mol) and the calculated CCSD(T)//M06-2x/aug-cc-pVDZ binding energy of dimer D1 (13.8 kJ/mol).

In this work no evidence of halogen-bonded structures was found, either experimentally or computationally.

Apparently, the lack of electron withdrawing substituents on the phenyl moiety minimizes the magnitude of the σ-hole, rendering the halogen bonding interactions weaker than π–stacking and CH/π interactions (Figure 1). From that point of view, fluorine substitution should increase the magnitude of the former. However, we note that a recent experimental study of C_6F_5X (X = Cl, Br, I) complexation in C_6D_6 solution using NMR spectroscopy found evidence for halogen bonding only in the case of X = I.[23]

In an effort to probe the excited state lifetime of the chlorobenzene clusters, we carried out R2C2PI experiments using the 266 nm output of a second Nd:YAG laser to ionize from the S_1 state. As mentioned above, ultrafast experiments have found a bi-exponential decay from the intermediate state, with a fast component on the order of 150-200 fs that was assigned to internal conversion to S_0 and a much slower (ns) component that was assigned to dissociation from highly excited levels of S_0. For the long lifetime component, there is an increase in lifetime with increasing cluster size, with the measured tetramer lifetime ~3.7 ns. Given the 5-8 ns pulse width of our lasers, we were unable to detect a difference in lifetime for the clusters as compared to the monomer. We did, however, confirm the short lifetime of the intermediate state, as R2C2PI signal could only be observed when the laser pulses were overlapped both temporally and spatially.

Finally, we note that the results found here are likely to be of general validity in understanding the similarly broad R2PI spectra that have been previously reported for other related systems, including not only toluene but other halobenzenes[62] and mixed halobenzene/benzene clusters.[70] Our results suggest that this broadening arises in large part from inhomogeneous sources, including the presence of multiple isomers and Franck-Condon activity associated with geometrical changes induced by electronic excitation, which is particularly important for the π-stacked clusters that display very low frequency intermolecular vibrations.

IV. CONCLUSIONS

Motivated by a desire to examine competitive noncovalent interactions in a prototypical system, we have examined the chlorobenzene monomer and clusters $(Clbz)_n$ with n = 2-4 using R2PI spectroscopy in concert with electronic structure calculations. The R2PI spectra of the clusters, obtained in the origin region of the S_0–S_1 ($\pi\pi^*$) state of the monomer, show a broad spectrum whose center is redshifted from the monomer absorption, and which is similar for all cluster sizes examined. These observations are explained with the aid of electronic structure calculations. For the dimer, calculations find five minimum energy structures, four π-stacked and one T-shaped structure bound through CH/π interaction. The calculated TDDFT spectra show that these isomers absorb over a broad range, and, in agreement with experiment, the calculated absorptions are redshifted with respect to the monomer transition. Due to the significant geometry change in the two electronic states, where electronic excitation induces a transition from a parallel displaced to sandwich structure with a reduced separation of the two monomers, significant FC activity is predicted in low frequency intermolecular modes of the complex.

For the trimer, six representative structures were found, displaying a combination of π-stacking and CH/π interactions. The calculated TDDFT spectra of these trimers are similar to those obtained for the dimers, consistent with the similarity of the experimental spectra for these clusters. Overall, our results show that the spectral broadening arises in large part from inhomogeneous sources, including the presence of multiple isomers and Franck-Condon activity associated with geometrical changes induced by electronic excitation. The latter is particularly important for the π-stacked structures, due to the presence of low frequency intermolecular modes.

Building upon these studies, a variety of additional experiments would aid in understanding the properties of the chlorobenzene clusters. Hole-burning experiments would help identify the spectral features associated with different ground state structures, while higher resolution mass-analyzed threshold ionization, MATI, or ZEKE spectroscopic methods are also attractive for application to this system. Finally, R2C2PI experiments with two tunable sources are attractive for probing the isomer dependence of the ionization potential, and unraveling contributions in the spectra from different isomers.

ACKNOWLEDGMENTS

Support of this research by the National Science Foundation (CHE-1010597) is gratefully acknowledged. This research was also supported in part by National Science Foundation Award Nos. OCI-0923037 "MRI: Acquisition of a Parallel Computing Cluster and Storage for the Marquette University Grid (MUGrid)" and CBET-0521602 "Acquisition of a Linux Cluster to Support College-Wide Research & Teaching Activities." This article is dedicated to Thomas J. Reid.

[1] M. Yamakawa, I. Yamada, and R. Noyori, Angew. Chem., Int. Ed. **40**, 2818 (2001).
[2] M. Nishio, Tetrahedron **61**, 6923 (2005).
[3] R. Bertani, P. Sgarbossa, A. Venzo, F. Lelj, M. Amati, G. Resnati, T. Pilati, P. Metrangolo, and G. Terraneo, Coor. Chem. Rev. **254**, 677 (2010).
[4] M. Nishio, J. Mol. Struct. **1018**, 2 (2012).
[5] S. J. Grabowski, Chem. Rev. **111**, 2597 (2011).
[6] A. C. Legon and D. J. Millen, Chem. Soc. Rev. **21**, 71 (1992).
[7] J. E. Del Bene and M. J. T. Jordan, Int. Rev. Phys. Chem. **18**, 119 (1999).
[8] G. C. Pimentel and A. L. McClellan, *The Hydrogen Bond* (Freeman, New York, San Francisco, 1960).
[9] P. Schuster, G. Zundel, and C. Sandorfy, *The Hydrogen Bond: Recent Developments in Theory and Experiments* (North-Holland, Amsterdam/New York, 1976).
[10] *206th American Chemical Society Meeting*, Chicago, Ill, 1993; D. A. Smith, and American Chemical Society. Division of Computers in Chemistry, *Modeling The Hydrogen Bond* (American Chemical Society, Washington, DC, 1994).
[11] M. Muraki, Protein Pept. Lett. **9**, 195 (2002).
[12] Y. Nakagawa, K. Irie, R. C. Yanagita, H. Ohigashi, and K. Tsuda, J. Am. Chem. Soc. **127**, 5746 (2005).
[13] K. Ramirez-Gualito, R. Alonso-Rios, B. Quiroz-Garcia, A. Rojas-Aguilar, D. Diaz, J. Jimenez-Barbero, and G. Cuevas, J. Am. Chem. Soc. **131**, 18129 (2009).
[14] M. Nishio, Phys. Chem. Chem. Phys. **13**, 13873 (2011).
[15] G. Cavallo, P. Metrangolo, T. Pilati, G. Resnati, M. Sansotera, and G. Terraneo, Chem. Soc. Rev. **39**, 3772 (2010).

[16]V. Amendola, L. Fabbrizzi, and L. Mosca, Chem. Soc. Rev. **39**, 3889 (2010).
[17]K. S. Thanthiriwatte, E. G. Hohenstein, L. A. Burns, and C. D. Sherrill, J. Chem. Theory Comput. **7**, 88 (2011).
[18]M. Nishio, Y. Umezawa, and M. Hirota, J. Synth. Org. Chem., Jpn. **55**, 2 (1997).
[19]P. Auffinger, F. A. Hays, E. Westhof, and P. S. Ho, Proc. Natl. Acad. Sci. U.S.A. **101**, 16789 (2004).
[20]A. R. Voth, F. A. Hays, and P. S. Ho, Proc. Natl. Acad. Sci. U.S.A. **104**, 6188 (2007).
[21]M. Nishio, M. Hirota, and Y. Umezawa, *The CH-[pi] Interaction: Evidence, Nature, and Consequences* (Wiley, New York, 1998).
[22]G. R. Desiraju and T. Steiner, *The Weak Hydrogen Bond: In Structural Chemistry and Biology* (Oxford University Press, Oxford, New York, 1999).
[23]Y. Zhang, B. M. Ji, A. M. Tian, and W. Z. Wang, J. Chem. Phys. **136**, 141101 (2012).
[24]C. Chipot, R. Jaffe, B. Maigret, D. A. Pearlman, and P. A. Kollman, J. Am. Chem. Soc. **118**, 11217 (1996).
[25]E. Arunan, G. R. Desiraju, R. A. Klein, J. Sadlej, S. Scheiner, I. Alkorta, D. C. Clary, R. H. Crabtree, J. J. Dannenberg, P. Hobza, H. G. Kjaergaard, A. C. Legon, B. Mennucci, and D. J. Nesbitt, Pure Appl. Chem. **83**, 1619 (2011).
[26]P. Metrangolo and G. Resnati, Science **321**, 918 (2008).
[27]D. Sredojevic, G. A. Bogdanovic, Z. D. Tomic, and S. D. Zaric, Cryst. Eng. Comm. **9**, 793 (2007).
[28]S. Zhu, C. Xing, W. Xu, G. Jin, and Z. Li, Cryst. Growth Des. **4**, 53 (2004).
[29]S. Zhu, C. Xing, W. Xu, and Z. Li, Tetrahedron Lett. **45**, 777 (2004).
[30]K. S. Law, M. Schauer, and E. R. Bernstein, J. Chem. Phys. **81**, 4871 (1984).
[31]D. W. Squire and R. B. Bernstein, J. Phys. Chem. **88**, 4944 (1984).
[32]C. A. Hunter and J. K. M. Sanders, J. Am. Chem. Soc. **112**, 5525 (1990).
[33]S. Tsuzuki, K. Honda, T. Uchimaru, M. Mikami, and K. Tanabe, J. Am. Chem. Soc. **122**, 3746 (2000).
[34]L. A. Burns, A. Vazquez-Mayagoitia, B. G. Sumpter, and C. D. Sherrill, J. Chem. Phys. **134**, 084107 (2011).
[35]T. Clark, M. Hennemann, J. S. Murray, and P. Politzer, J. Mol. Model. **13**, 291 (2007).
[36]P. Politzer, P. Lane, M. C. Concha, Y. Ma, and J. S. Murray, J. Mol. Model. **13**, 305 (2007).
[37]P. Politzer, J. S. Murray, and M. C. Concha, J. Mol. Model. **13**, 643 (2007).
[38]P. Politzer, *Halogen Bonding: Fundamentals and Applications*, Structure and Bonding 126, edited by P. Metrangolo and G. Resnati (Springer, New York, 2008).
[39]M. O. Sinnokrot and C. D. Sherrill, J. Phys. Chem. A **108**, 10200 (2004).
[40]A. L. Ringer, M. S. Figgs, M. O. Sinnokrot, and C. D. Sherrill, J. Phys. Chem. A **110**, 10822 (2006).
[41]M. O. Sinnokrot and C. D. Sherrill, J. Phys. Chem. A **110**, 10656 (2006).
[42]C. D. Sherrill, B. G. Sumpter, M. O. Sinnokrot, M. S. Marshall, E. G. Hohenstein, R. C. Walker, and I. R. Gould, J. Comput. Chem. **30**, 2187 (2009).
[43]E. Arunan and H. S. Gutowsky, J. Chem. Phys. **98**, 4294 (1993).
[44]V. Chandrasekaran, L. Biennier, E. Arunan, D. Talbi, and R. Georges, J. Phys. Chem. A **115**, 11263 (2011).
[45]P. Hobza, H. L. Selzle, and E. W. Schlag, Chem. Rev. **94**, 1767 (1994).
[46]S. Tsuzuki, K. Honda, T. Uchimaru, M. Mikami, and K. Tanabe, J. Phys. Chem. A **106**, 4423 (2002).
[47]S. Tsuzuki, K. Honda, T. Uchimaru, M. Mikami, and K. Tanabe, J. Am. Chem. Soc. **124**, 104 (2002).
[48]S. Tsuzuki, T. Uchimaru, K. Sugawara, and M. Mikami, J. Chem. Phys. **117**, 11216 (2002).
[49]S. E. Wheeler, J. Am. Chem. Soc. **133**, 10262 (2011).
[50]S. E. Wheeler and K. N. Houk, J. Am. Chem. Soc. **130**, 10854 (2008).
[51]Y. X. Lu, J. W. Zou, Y. H. Wang, and Q. S. Yu, Chem. Phys. **334**, 1 (2007).
[52]L. Cheng, M. Y. Wang, Z. J. Wu, and Z. M. Su, J. Comput. Chem. **28**, 2190 (2007).
[53]Y. X. Lu, J. W. Zou, Y. H. Wang, Y. J. Jiang, and Q. S. Yu, J. Phys. Chem. A **111**, 10781 (2007).
[54]P. Metrangolo, F. Meyer, T. Pilati, G. Resnati, and G. Terraneo, Angew. Chem., Int. Ed. **47**, 6114 (2008).
[55]P. Metrangolo, H. Neukirch, T. Pilati, and G. Resnati, Acc. Chem. Res. **38**, 386 (2005).
[56]E. Parisini, P. Metrangolo, T. Pilati, G. Resnati, and G. Terraneo, Chem. Soc. Rev. **40**, 2267 (2011).
[57]P. Politzer, J. S. Murray, and T. Clark, Phys. Chem. Chem. Phys. **12**, 7748 (2010).
[58]B. K. Liu, B. X. Wang, Y. Q. Wang, and L. Wang, Chem. Phys. Lett. **477**, 266 (2009).
[59]T. M. Di Palma, A. Bende, and A. Borghese, Chem. Phys. Lett. **495**, 17 (2010).
[60]A. Musgrave and T. G. Wright, J. Chem. Phys. **122**, 074312 (2005).
[61]S. Ishikawa, T. Ebata, H. Ishikawa, T. Inoue, and N. Mikami, J. Phys. Chem. **100**, 10531 (1996).
[62]K. Rademann, B. Brutschy, and H. Baumgartel, Chem. Phys. **80**, 129 (1983).
[63]U. Dimopoulouradem ann, K. Rademann, P. Bisling, B. Brutschy, and H. Baumgartel, Ber. Bunsenges. Phys. Chem. Chem. Phys. **88**, 215 (1984).
[64]U. Even, K. Rademann, J. Jortner, N. Manor, and R. Reisfeld, Phys. Rev. Lett. **52**, 2164 (1984).
[65]T. Smith, L. V. Slipchenko, and M. S. Gordon, J. Phys. Chem. A **112**, 5286 (2008).
[66]R. Leist, J. A. Frey, P. Ottiger, H. M. Frey, S. Leutwyler, R. A. Bachorz, and W. Klopper, Angew. Chem., Int. Ed. **46**, 7449 (2007).
[67]R. Leist, J. A. Frey, and S. Leutwyler, J. Phys. Chem. A **110**, 4180 (2006).
[68]P. Hobza, V. Spirko, Z. Havlas, K. Buchhold, B. Reimann, H. D. Barth, and B. Brutschy, Chem. Phys. Lett. **299**, 180 (1999).
[69]P. Hobza, H. L. Selzle, and E. W. Schlag, J. Chem. Phys. **99**, 2809 (1993).
[70]W. Y. Lu, Y. H. Hu, Z. Y. Lin, and S. H. Yang, J. Chem. Phys. **104**, 8843 (1996).
[71]J. H. Yeh, T. L. Shen, D. G. Nocera, G. E. Leroi, I. Suzuka, H. Ozawa, and Y. Namuta, J. Phys. Chem. **100**, 4385 (1996).
[72]K. Sugawara, J. Miyawaki, T. Nakanaga, H. Takeo, G. Lembach, S. Djafari, H. D. Barth, and B. Brutschy, J. Phys. Chem. **100**, 17145 (1996).
[73]N. Yamamoto, K. Hino, K. Mogi, K. Ohashi, Y. Sakai, and H. Sekiya, Chem. Phys. Lett. **342**, 417 (2001).
[74]N. Yamamoto, K. Ohashi, K. Hino, H. Izutsu, K. Mogi, Y. Sakai, and H. Sekiya, Chem. Phys. Lett. **345**, 532 (2001).
[75]Y. Numata, Y. Ishii, M. Watahiki, I. Suzuka, and M. Ito, J. Phys. Chem. **97**, 4930 (1993).
[76]D. E. Bergeron, V. L. Ayles, O. J. Richards, and T. G. Wright, Chem. Phys. Lett. **430**, 282 (2006).
[77]J. L. Durant, D. M. Rider, S. L. Anderson, F. D. Proch, and R. N. Zare, J. Chem. Phys. **80**, 1817 (1984).
[78]B. D. Koplitz and J. K. Mcvey, J. Chem. Phys. **80**, 2271 (1984).
[79]B. D. Koplitz and J. K. Mcvey, J. Chem. Phys. **81**, 4963 (1984).
[80]D. M. Szaflarski, J. D. Simon, and M. A. Elsayed, J. Phys. Chem. **90**, 5050 (1986).
[81]J. Murakami, K. Kaya, and M. Ito, J. Chem. Phys. **72**, 3263 (1980).
[82]E. J. Bieske, M. W. Rainbird, and A. E. W. Knight, J. Chem. Phys. **90**, 2068 (1989).
[83]K. Tonokura, T. Nakamura, and M. Koshi, Anal. Sci. **19**, 1109 (2003).
[84]See supplementary material at http://dx.doi.org/10.1063/1.4765102 for X figures of additional data.
[85]V. L. Ayles, L. G. Muzangwa, and S. A. Reid, Chem. Phys. Lett. **497**, 168 (2010).
[86]L. G. Muzangwa, V. L. Ayles, S. Nyambo, and S. A. Reid, J. Mol. Spectrosc. **269**, 36 (2011).
[87]C. Tao, C. Mukarakate, Y. Mishchenko, D. Brusse, and S. A. Reid, J. Phys. Chem. A **111**, 10562 (2007).
[88]M. J. Frisch, G. W. Trucks, H. B. Schlegel *et al.*, GAUSSIAN 09, Revision A.1, Gaussian, Inc., Wallingford, CT, 2009.
[89]Y. Zhao and D. G. Truhlar, Theor. Chem. Acc. **120**, 215 (2008).
[90]A. Dreuw, J. L. Weisman, and M. Head-Gordon, J. Chem. Phys. **119**, 2943 (2003).
[91]J. D. Chai and M. Head-Gordon, J. Chem. Phys. **131**, 174105 (2009).
[92]T. Yanai, D. P. Tew, and N. C. Handy, Chem. Phys. Lett. **393**, 51 (2004).
[93]M. J. G. Peach, T. Helgaker, P. Salek, T. W. Keal, O. B. Lutnaes, D. J. Tozer, and N. C. Handy, Phys. Chem. Chem. Phys. **8**, 558 (2006).
[94]N. Mardirossian, J. A. Parkhill, and M. Head-Gordon, Phys. Chem. Chem. Phys. **13**, 19325 (2011).
[95]H. J. Heger, U. Boesl, R. Zimmermann, R. Dorfner, and A. Kettrup, Eur. Mass Spectrom. **5**, 51 (1999).
[96]H. J. Heger, R. Zimmermann, R. Dorfner, M. Beckmann, H. Griebel, A. Kettrup, and U. Boesl, Anal. Chem. **71**, 46 (1999).

[97]P. Imhof and K. Kleinermanns, Chem. Phys. **270**, 227 (2001).
[98]K. Walter, K. Scherm, and U. Boesl, J. Phys. Chem. **95**, 1188 (1991).
[99]S. M. Cybulski and M. L. Lytle, J. Chem. Phys. **127**, 141102 (2007).
[100]P. Jurecka, J. Sponer, J. Cerny, and P. Hobza, Phys. Chem. Chem. Phys. **8**, 1985 (2006).
[101]K. Diri and A. I. Krylov, J. Phys. Chem. A **116**, 653 (2012).
[102]J. C. Amicangelo, J. Phys. Chem. A **109**, 9174 (2005).
[103]C. Western, PGOPHER, *a Program for Simulating Rotational Structure* (University of Bristol, 2010).
[104]T. P. Tauer and C. D. Sherrill, J. Phys. Chem. A **109**, 10475 (2005).